ACS OMEGA

Open Access

http://pubs.acs.org/journal/acsodf

Article

Development and Characterization of Biodegradable Polyurethane-Urea-Based Hydrogels for the Prevention of Postoperative Peritoneal Adhesions

Lana Kortenbrede,[⊥] Johanna Heider,[⊥] Heike Heckroth, Marc Leimenstoll, Heiko Steuer, Jan Sütterlin, Frank Weise, and Tobias Hokamp*

Cite This: *ACS Omega* 2024, 9, 34008−34020

Read Online

ACCESS | Metrics & More | Article Recommendations | Supporting Information

ABSTRACT: Postoperative peritoneal adhesions occur after more than 60% of abdominal surgeries and can cause severe long-term side effects, such as chronic pain, infertility, and intestinal obstructions. However, currently available products for adhesion prophylaxis often lack efficiency or are too heavy to handle. Hydrogels are promising materials to be used for adhesion prevention as they show good mechanical stability and biocompatibility. Herein, we present a novel two-component sprayable, biodegradable, fast-curing, and shape-adaptive polyurethane urea (PUU) hydrogel system and the establishment of a full characterization approach to investigate its suitability for adhesion prophylaxis according to predefined chemical, mechanical, and biological criteria. We demonstrate that this PUU hydrogel system exhibits a fast-curing behavior, is resilient toward mechanical forces, is biocompatible, and reveals a degradation behavior within a desired time frame to reliably avoid the formation of adhesions. In addition, the PUU hydrogel system functions as an effective barrier for invading cells *in vitro*. Overall, we propose a guideline for the development and *in vitro* characterization of synthetic hydrogels for application in minimally invasive adhesion prophylaxis.

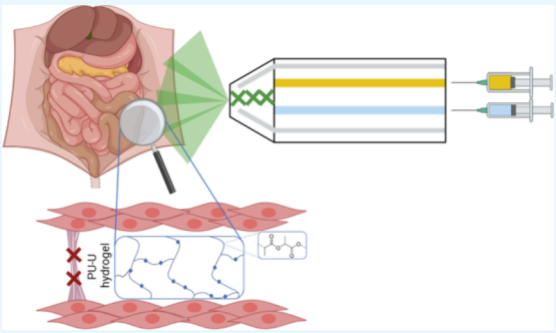

INTRODUCTION

In many areas of the human body, hydrogels are encountered, such as in extracellular matrices or as tendons, which are composed of natural macromolecules like collagen or gelatin.[1] In recent years, the use of synthetic hydrogels gained more interest, and they are used nowadays in various applications, such as wound dressings,[2] contact lenses,[3] or for drug delivery systems,[4] as well as tissue engineering[1] and adhesion prophylaxis.[5] According to the classical definition, a hydrogel is a three-dimensional network capable of storing a large amount of water without going into solution itself.[6] Because of the three-dimensional arrangement, hydrogels also have certain mechanical properties that make them ideal materials that possess little solid content but still comprise mechanical stability while causing reduced irritating reactions when embedded into living organisms.[7] Therefore, hydrogels promise high biocompatibility.[8]

Adhesion prophylaxis can be seen as a special form of an implantable wound dressing that is useful for the prevention of postoperative adhesions. In the literature, a widely varying incidence of outgrowth of postoperative adhesions is reported, affecting 63−97% of all abdominal surgeries (laparotomy).[9−11] The detailed formation process of adhesions has been previously described.[12,13] The most crucial step in adhesion formation is migration of fibroblasts into the wounded area. Prior to the application of adhesion barriers, the formation of postoperative adhesions could not be prevented simply by professional precautions taken during the operation, as it is caused by the wound healing process in response to tissue injury during surgery. Although such adhesions partially regress, the majority of patients are affected by long-term side effects such as chronic pain, intestinal obstruction, or, in the case of women, infertility.[12] To prevent postoperative adhesions, adhesion prophylaxis can be applied to an affected tissue or organ at the end of the surgical intervention in the form of a coating for the intraabdominal tissue. In recent years, various products have been introduced to the market. However, these products often show insufficient efficacy or are cumbersome to handle.[14] Common materials used for adhesion prophylaxis products include biological compounds such as potato starch or hyaluronic acid (HA), modified biological compounds such as carboxy methyl cellulose

Received: May 14, 2024
Revised: July 3, 2024
Accepted: July 11, 2024
Published: July 25, 2024

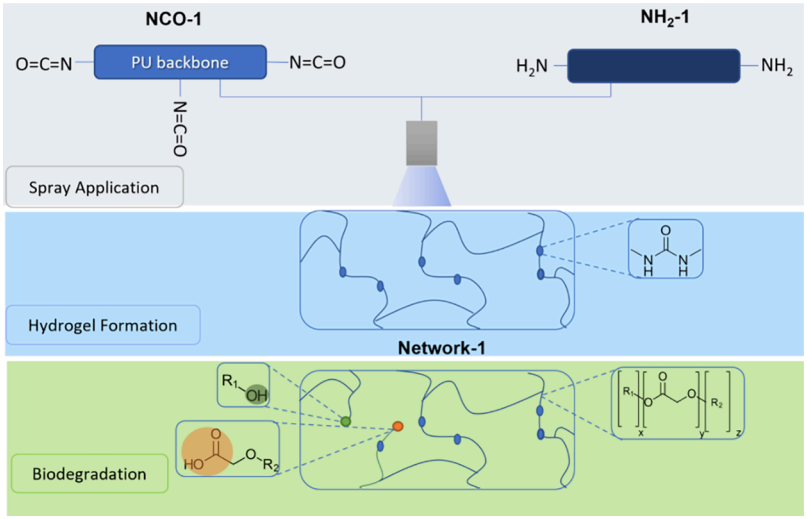

Figure 1. General concept for the targeted application of sprayable hydrogels as adhesion prophylaxis. Single components **NCO-1** and **NH_2-1** were provided as aqueous solutions being mixed during the spray application. The hydrogel formation occurs in situ in <60 s on the tissue where it is applied on. The implementation of degradable sites into the prepolymer backbone allows degradation of the hydrogel network to avoid a second surgery necessary for the removal of the barrier.

(CMC) or polylactic acid (PLA), and even entirely synthetic compounds such as expanded polytetrafluorethylene (ePTFE).[15−18]

Herein, we thoroughly report on the features and characteristics of a novel sprayable two-component (2K) polyurethane urea (PUU) hydrogel system[19] as well as an assessment regarding its potential to be used as a biocompatible adhesion prophylaxis according to EN ISO 10993 ("Biological evaluation of medical devices"). Because current literature lacks a defined approach for the investigation of such a system, we herein propose how to characterize a material for this kind of application with focus on viscoelastic properties, curing behavior, pH value, mechanical properties, cytotoxicity, pyrogenicity, biodegradation, and *in vitro* efficacy. This project therefore depicts a guideline leading from the initial synthesis of raw materials for hydrogel manufacturing to advanced *in vitro* efficacy testing and therefore covers a large fraction of the value chain for such a product.

A general concept for the application of our novel 2K PUU hydrogel system is depicted in Figure 1.

MATERIALS

Raw Materials. Jeffamine ED2003 was purchased from Huntsman, hexamethylene diisocyanate and polyether-1 were provided by Covestro Deutschland AG, ethylene oxide (EO) was purchased from GHC Gerling Holz, propylene oxide (PO) was purchased from Chemogas, dilactide (>99%) and dibutyl phosphate (≥97%) were purchased from Sigma-Aldrich, and 0.1 M HCl was purchased from Honeywell Fluka. All chemicals were used without further purification.

For synthesis details of polyol and prepolymer, see the Supporting Information.

Preparation of Components. *Preparation of the NH_2 Component.* Jeffamine ED2003 (**NH_2-1**) (1.94 g, 0.0019 eq., 0.00095 mol) was weighed into a flask and added up with 2.11 g aqueous HCl (0.1 M) and 8.45 g double-distilled water (ddH_2O). The solution was stirred for 30 min until Jeffamine was fully dissolved.

Preparation of the NCO Component. **NCO-1** (3.75 g, 0.0023 equiv, 0.00077 mol) was weighed into a mixing cup and filled up to 25 g with ddH_2O. The solution was mixed for 30 s. Afterward, the solution was directly filled into a cartridge of the glue gun, and mixing experiments were conducted immediately, as described below.

Preparation of Hydrogels for pH Measurements and for Mechanical Testing. A glue gun (DMA 51-00-10) equipped with an appropriate cartridge comprising two chambers (AB 050-02-10-33) from AdChem was used for the application of the two-component hydrogel. The volumes of the two chambers of the cartridges were 25 mL (provision of **NCO-1**) and 12.5 mL (provision of **NH_2-1**). Cartridges were prefilled, and experiments started immediately. A static mixer (AdChem, MBH 05-20T) was used for the mixing process. Single solutions were dispensed with a constant volume ratio of 2:1 (NCO/NH_2) within ∼25 s.

Preparation of Hydrogels for Rheology and Cellular Assays. Preparation of hydrogels for rheology measurements, cell invasion assay, cell adhesion assay, and cytotoxicity assay was performed by pipetting. **NCO-1** was mixed with ddH_2O (15 wt %) by stirring on a magnetic plate for 1−2 min. Care was taken that prepolymer/H_2O solutions were used within a maximum of 10 min after preparation as they will otherwise solidify afterward. The **NH_2-1** solution was transferred either into a well or onto the rheometer plate and combined with the prepolymer/H_2O mixture, at a ratio of 1:2, by rapidly pipetting up and down (two to three times). Polymerization of the hydrogels occurred within a few seconds.

METHODS

^{1}H NMR. ^{1}H NMR spectra (600 MHz) were recorded in d_6DMSO (polyol) and $CDCl_3$ (prepolymer **NCO-1**) using a Bruker AV III HD 600.

^{13}C NMR. ^{13}C NMR spectra (151 MHz) were recorded in d_6DMSO (polyol) and $CDCl_3$ (prepolymer **NCO-1**) using a Bruker AV III HD 600.

Hydroxyl Value Determination. The hydroxyl value was determined according to EN ISO 4629-2.

Total Acidic Value Determination. The total acidic value was determined according to EN ISO 2114:2000.

https://doi.org/10.1021/acsomega.4c04577
ACS Omega 2024, 9, 34008−34020

Amine Value Determination. The amine value represents the quantity of KOH in milligrams equivalent to one gram of a substance and was determined according to DIN 16945.

NCO Content Determination. The NCO content was determined according to EN ISO 14896.

NCO Conversion. FT-IR/ATR spectroscopy was used for the determination of the NCO conversion during the curing reaction. Experiments were carried out on a Bruker Vertex 70 instrument with an attenuated total reflection (ATR) zinc selenide crystal. A baseline correction (rubber band method with anchor points at 983, 1011, 1192, 1830, 2620, and 3984 cm^{-1}) was performed for all spectra, and a normalization method was applied using the peak area between 3050 and 3750 cm^{-1}.

pH Measurements. pH measurements were conducted for 30 min and were carried out using a Knick Portamess 911 pH. The 2K system was applied in a beaker equipped with a pH electrode inside. The electrode was immersed in both **NCO-1** and **NH_2-1** solutions, and measurements started immediately, including recording of data during the time of application. The pH was measured for 30 min, and pH values were recorded at different time intervals depending on the speed of pH change.

Mechanical Properties. Tensile tests were carried out using a Zwick Retro tensometer with a 2 kN load cell at a test speed of 200 mm min^{-1} and a preload of 0.002 N mm^{-2} at 23.6 °C and 47.9% relative humidity. Four S-2 test specimens, dog bones, were punched out from freshly prepared cured hydrogels, and measurements were performed.

Viscosity Determination. The viscosity measurements of the raw materials were conducted according to EN ISO 3219. A rotational viscometer from Anton Paar (MCR301) was used for the determination. Measurements were carried out using a cone−plate geometry (α = 5°) configuration with a quartz glass plate and a disposable aluminum stamp (d = 25 mm). The temperature was set to a defined value, and the shear rate was set to 50 Hz. A sample was applied on the surface of the heater, and measurements were started immediately for 40 s with one data point every 2 s. Twenty single values were recorded, whereas the last point was chosen as reference for effective viscosity.

Rheological Characterization. A calibrated Kinexus pro rheometer (Malvern Instruments, Herrenberg, Germany) was used for the analysis. The analyses were conducted by placing 80 μL of the diamine-based curing agent on the bottom plate of the rheometer. Subsequently, a freshly prepared solution of the prepolymer in ddH_2O (15% w/w, 200 μL) was added to the curing agent, and all components were quickly mixed by pipetting. The upper plate (stainless steel, 20 mm diameter) was immediately adjusted, leaving a gap of 600 μm. Different measurements were carried out at 37 °C to analyze the gelation and deformation behavior of the PUU hydrogel. Oscillatory time sweeps were started with a predefined frequency (f = 1 Hz) and a controlled shear strain (γ = 1%). The storage modulus (G') and loss modulus (G'') were detected every 8 s over a period of 65 min. Moreover, frequency sweeps were conducted by applying decreasing frequencies from 10 to 0.1 Hz using a constant shear strain (γ = 1%). Finally, amplitude sweeps were performed using increasing shear strains from 0.1 to 1000% in combination with a constant frequency (f = 1 Hz).

Data are either presented as a time course of G' and G'' (time sweep), as a function of shear strain plotted against G' and G'' (amplitude sweep), or frequency plotted against G' and G'' (frequency sweep). The point of gelation in a time sweep is an important criterium for analyzing the gelation behavior of a material and is reached when $G' = G''$. Moreover, the linear viscoelastic region (LVER) is a crucial parameter to verify that the oscillatory time sweeps were conducted using a nondestructive degree of deformation. The LVER is defined as the region where G' and G'' are independent of the applied shear strain. Hence, within the LVER, microstructures remain intact, and disruptions can be immediately recovered. All rheological analyses were measured in triplicates.

Degradation Studies Using Gravimetry and Gel Permeation Chromatography. Hydrolytic degradation studies of the hydrogels were conducted based on EN ISO 10993-13 ("Biological evaluation of medical devices − Part 13: Identification and quantification of degradation products from polymeric medical devices"). A hydrogel was prepared by mixing the diamine-based curing agent and the prepolymer mixed with water (15% w/w, 1:2) using spray application. Samples of the gels were cut with the help of a round cutter (diameter: 3.5 cm) to result in small samples with weights between 630 and 1200 mg and thicknesses between 0.7 and 1.2 mm. The degradation study of the freshly prepared hydrogels was performed at 37 °C by immersing each gel sample in Dulbecco's phosphate buffered saline (DPBS), 1×, no calcium, no magnesium, Thermo Fisher Scientific #14190169 with a mass/volume ratio of 1:15. The hydrogel samples were removed from the solution after predetermined incubation times, salts were removed by washing the gels three times with water (initial mass/volume ratio = 1:15), and the samples were dried under a vacuum at 40 °C for 24 h to determine the weight of the dried hydrogel after incubation. The weights of the dried hydrogels before and after incubation were compared. The weight of the dried hydrogel before incubation was not experimentally determined but theoretically calculated by considering the initial weight of the freshly prepared hydrogel and the theoretical weight loss during the drying process of the hydrogel under vacuum. The initial weight loss of the freshly hydrogel during the drying process was experimentally determined in a preliminary experiment. Moreover, degradation products in the supernatant were analyzed regarding the molecular weight distribution by employing gel permeation chromatography (GPC). GPC analyses of the undiluted samples were performed on a Malvern Panalytical OMNISEC system (OMNISEC REVEAL & OMNISEC RESOLVE) using multidetection (light scattering, viscometer, refractive index). $NaNO_3$ (0.2 M) in ddH_2O acidified with AcOH (0.25%, pH = 3.0) was used as eluent. Separation was performed using a PSS 5μm NOVEMA MAX 100 Å column (8 × 300 mm) with a flow rate of 1.0 mL min^{-1} at 35 °C. Molecular weight parameters M_W and dispersity ($Đ_M$; a measure that describes the spread of the molecular weight distribution in the polymer sample) were calculated after universal calibration of the detectors using the polysaccharide pullulan (Malvern Panalytical, #TDS3030) as calibration standard and dextran (Malvern Panalytical, #TDS3030) as verification standard. The refractive index increment of the degradation products (dn/dc = 0.139) was determined using a mixture of degradation products of a known concentration after the removal of salts via dialysis. All experiments were conducted in triplicates.

Pyrogen Testing. Hydrogels were polymerized in a 96-well plate (30 μL) via pipetting. Subsequently, the gels were covered with either 50 μL limulus amebocyte lysate (LAL)

https://doi.org/10.1021/acsomega.4c04577
ACS Omega 2024, 9, 34008−34020

reagent water (LRW, Charles River) or different concentrations of endotoxins (0.1−500 EU mL^{-1}) to identify possible low endotoxin recovery (LER) or binding of endotoxins to the hydrogel resulting in a masking of endotoxins. After 23 h of incubation at 37 °C, human monocytes (PyroMAT Cells, Mono-Mac-6, Merck) were added, and the resulting mixture was incubated for another 23 h at 37 °C. Supernatants were then either directly transferred to an IL-6 ELISA microplate (PyroMAT Kit, Merck) or, for those with high concentrations of spiked endotoxins, diluted before transfer. The initial production of the cytokine (interleukin IL-6) was quantified by a standard ELISA (PyroMAT Kit, Merck) according to the manufacturer's instructions. Briefly, an IL-6 conjugate (human IL-6 specific antibody conjugated to horseradish peroxidase) was added to each well filled with supernatant, and the ELISA plate was incubated for 2 h at room temperature. After washing the wells four times, a substrate solution (hydrogen peroxide and tetramethylbenzidine) was added for 30 min at room temperature in the dark. A stop solution (2 N sulfuric acid) was added subsequently, and the solutions were thoroughly mixed by pipetting up and down. Immediately afterward, the optical density was determined using a microplate reader (ELx808, BioTek) set to 450 nm with wavelength corrections set to 630 nm.

Cell Culture of A549 Cell Line. A genetically modified A549 human lung carcinoma cell line was used for cytotoxicity testing, cell invasion, and cell adhesion assays. The modified cell line stably expresses vimentin-GFP and actin-RFP. Therefore, puromycin (1 $\mu g\ mL^{-1}$, Thermo Fisher Scientific #A1113803) and hygromycin (80 $\mu g\ mL^{-1}$, Carl Roth #CP12.1) were added to the culture media to ensure constant selection of transgene-expressing cells. Cells were cultured in DMEM/F12 (Thermo Fisher Scientific #11320033) + 10% FKS (Thermo Fisher Scientific #A5256701) + 1% L-glutamine (Thermo Fisher Scientific #25030032) + 1% penicillin/streptomycin (Thermo Fisher Scientific #15070063) and enzymatically passaged with trypsin-EDTA (0.025%, Thermo Fisher Scientific #25300054) at a minimum ratio of 1:10.

Cytotoxicity Test. The cytotoxicity of PUU hydrogels was assessed using an MTT (3-(4,5-dimethylthiazol-2-yl)-2,5-diphenyltetrazolium bromide) assay based on the recommendations for *in vitro* cytotoxicity evaluation of medical devices in ISO 10993-5. To generate extracts of PUU hydrogels, gels with a total mass of 5 g were obtained by pipetting. Gel pieces were placed in 25 mL of cell culture medium and incubated at 37 °C and 5% CO_2 for 7 or 14 days on an orbital shaker. At the end of the incubation period, gel extracts were filtered through cell strainers (SPL, 100 μm pore size, #93100) to remove any remaining larger gel fragments. Fresh gel extracts were immediately used for experiments. Prior to treatment, 1×10^4 A549 cells were seeded per well of a 96-well plate in a culture medium. When cells reached a confluence of approximately 80%, the medium was removed, and the cells were treated with 100 μL of gel extracts or control substances for 24 h at 37 °C, 5% CO_2. Gel extracts were diluted in culture medium and tested at four concentrations: undiluted, 1:2, 1:5 and 1:10. Staurosporine (10 μM, Sigma-Aldrich #S5921) was used as a positive control, and the cell culture medium was used as a negative control. MTT assays were conducted using the MTT Cell Growth Assay Kit (Sigma-Aldrich #CT02) according to the manufacturer's instructions. Absorbance of formazan was measured at 570 nm with a reference wavelength of 630 nm using a Spark microplate reader (TECAN, Switzerland). All conditions were tested in technical triplicates and three independent biological replicates.

HPRT Assay. To test for potentially mutagenic effects of hydrogel degradation products, a hypoxanthine−guanine phosphoribosyltransferase (HPRT) assay based on the recommendations for mutagenicity testing of medical devices in ISO 10993-3 was performed using the Chinese hamster ovary cell line CHO-K1. Gel extracts were obtained as described above by incubation of gels in CHO-K1 culture medium (Ham's F-12 Nutrient mix (Thermo Fisher Scientific #21765037) + 10% fetal calf serum (FCS) + 1% L-glutamine + 1% penicillin/streptomycin) for 7 days. To cleanse the pre-existing mutants, CHO-K1 cells were cultured in hypoxanthine−aminopterin−thymidine (HAT)-supplemented media for 3 days (Sigma-Aldrich #H0262). Afterward, cells were cultured in hypoxanthine−thymidine (HT)-containing media (Sigma-Aldrich #H0137) for 24 h before transitioning back to the standard culture medium. At the start of the experiment, two 100 mm Petri dishes with 1×10^6 cells per dish were seeded for each treatment condition. Once the cells reached approximately 80% confluence, they were treated for 4 h with the substances listed in Table S2. The culture medium was used as the diluent and negative control. The mutagenic substances ethyl methanesulfonate (CAS-no.: 62-50-0, Sigma-Aldrich #M0880) and benzo[*a*]pyrene (CAS-no.: 50-32-8, Sigma-Aldrich #CRM40071) were used as positive controls. For metabolic activation, liver extract S9 (Sigma-Aldrich no. S2067) was supplemented at a final concentration of 2%. After treatment, the cells were washed with DMEM/F-12 and cultured for 7 days in a regular culture medium. During this culture period, cells were split regularly to avoid changes of pH. For splitting, cells were detached using trypsin-EDTA (0.025%), and 1×10^6 viable cells were seeded in two Petri dishes for every condition. After 7 days of culturing, the cells were detached, and 2×10^5 cells were sparsely seeded in two Petri dishes per treatment condition to avoid metabolic cooperation. The cells were then cultured in medium containing 25 $\mu g\ mL^{-1}$ of the selective agent 6-thioguanine (Sigma-Aldrich no. A4882) for 7 to 12 days. Once colonies with a minimum size of 10 cells appeared, which indicates mutations in the *HPRT* gene, the experiment was terminated. Cells were fixed with 4% paraformaldehyde in PBS for 20 min at room temperature, washed three times with PBS, and stained with 0.1% crystal violet for 30 min at room temperature. Afterward, cells were again washed three times with PBS, and stained colonies were counted using the Fiji open-source software package.

Adhesion Assay. To test the capacity of cells to adhere to the surface of PUU hydrogels, adhesion assays were performed. To ensure that the gel surface for adhesion experiments was as straight as possible, the μ-Slide 15 well 3D from ibidi (no. 81501) was used. Gels with a total volume of 10 μL were generated in the lower chambers of the wells by pipetting. The undiluted extracellular matrix-based hydrogel Matrigel (Corning no. 356234) was used as a positive control for surface cell adhesion. Matrigel gels were incubated at 37 °C for 30 min until polymerized, and 5×10^3 A549 cells were seeded on top of each gel in 40 μL of the culture medium. The cells were incubated for 48 h or 7 days without any further medium changes. After the incubation period, the medium was removed and replaced with a fresh medium to eliminate unattached or dead cells. Adherent cells were imaged using the spinning disk confocal microscope Cell Observer SD (Zeiss, Germany). Tile

https://doi.org/10.1021/acsomega.4c04577
ACS Omega 2024, 9, 34008−34020

imaging of the entire gel surface with adherent RFP-positive A549 cells was performed with a 10× objective.

For quantification of adherent cells, particle detection was performed by using Fiji. Images were converted to 16-bit grayscale, and a fluorescence and particle size threshold for object detection was defined, which was kept constant within individual biological replicates. Data were obtained from three independent biological replicates.

Invasion Assay. Invasion assays were conducted to assess the capacity of cells to invade or transverse the hydrogels. Gels with a total volume of 60 μL were generated by pipetting in 24-well Thincerts with 8 μm pore size (Greiner, #662638). Matrigel, diluted in DMEM/F12 to a protein concentration of 1 mg mL^{-1}, was used as a positive control and polymerized at 37 °C for 30 min. A total of 5×10^4 A549 cells were seeded on top of each gel in a starvation medium with low FCS concentration (DMEM F/12 + 0.5% FCS + 1% L-glutamine + 1% penicillin/streptomycin). The lower chamber was filled with a stimulation medium containing a high FCS concentration (DMEM F/12 + 20% FCS + 1% L-glutamine + 1% penicillin/streptomycin), to attract migrating cells to the lower chamber, thereby transversing the gels. The cultures were incubated for either 4 or 7 days at 37 °C and 5% CO_2, and the medium was changed daily to maintain the stimulating serum gradient. After the incubation period, cells that had transversed the gel and the underlying porous membrane were imaged with the spinning disk confocal microscope Cell Observer SD. To this end, RFP-positive cells on the entire membrane of each Thincert were imaged using the tiles option with a 10× objective. Invasive cells were quantified using Fiji as described above. Data were obtained from three independent biological replicates.

RESULTS AND DISCUSSION

NCO Conversion during Curing Reaction. The formation of the presented 2K hydrogel system follows the well-established curing technology based on the reaction of isocyanates (NCO) and primary amines (NH_2), yielding urea groups as cross-links (Scheme S1). The NCO component (**NCO-1**) is an isocyanate-terminated prepolymer comprising a large macromolecular, EO rich backbone with additional PO and dilactide units, with a functionality of $f = 3$ and an equivalent weight of 1457 g $equiv^{-1}$. The NH_2 component (**NH_2-1**) comprises an EO rich macromolecular backbone with $f = 2$ and an equivalent weight of 1021 g $equiv^{-1}$. Both components, **NCO-1** and **NH_2-1**, are provided as aqueous solutions, whereas the **NH_2-1** solution additionally contains hydrochloric acid (HCl) as a buffering agent in a concentration so that 15 mol % of the amine groups are protonated. This buffer is important to reach a physiological pH after curing of the hydrogel and does not strongly influence the curing behavior. According to Stockmayer, primary cross-linking for such systems occurs with indices (NCO/NH_2 ratios) below 2.0.[20] Therefore, primary gelation was well ensured by setting the index to 1.2. Postcuring of the residual NCO groups eventually yields the completely cross-linked hydrogel.

NCO conversion during the curing reaction was investigated via IR measurement and is depicted in Figure 2, clearly showing an initial NCO conversion of 75% at $t = 0$, which is probably caused by the reaction of **NCO-1** and **NH_2-1** during the initial mixing step and time lag of ∼20 s until data were recorded. NCO conversion at 127 s is still at 75% and increases after this time interval. Full NCO conversion is reached after

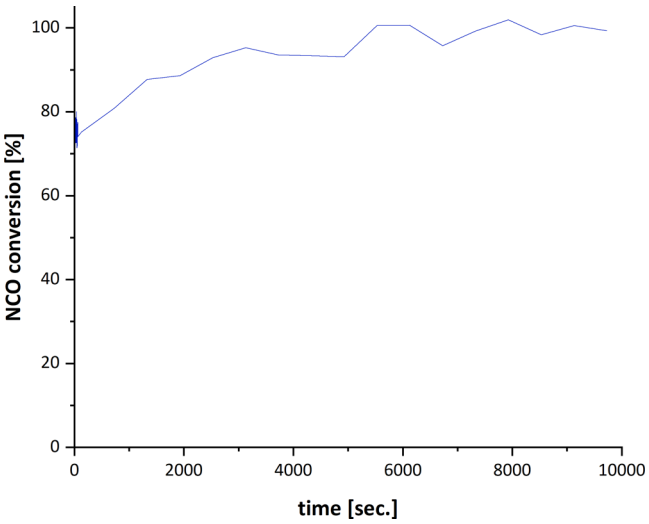

Figure 2. NCO conversion during the hydrogel curing reaction as a function of time. Reaction of **NH_2-1** and **NCO-1** during the initial mixing step and time lag between mixing and data recording cause 75% NCO conversion at $t = 0$. A 100% NCO conversion is reached after 92 min. NCO conversion was determined via IR measurements during the curing reaction by the integration of the band characteristic for an isocyanate group (2265 cm^{-1}).

92 min. The remaining NCO groups after the initial cross-linking reaction will predominantly react with H_2O under elimination of CO_2 to yield primary amines. Reactions between NCO and urea are not expected as the relative reaction rate of 1 has been reported for NCO/H_2O as compared to 0.15 for NCO/urea.[21] Moreover, the reactivity of **NCO-1** toward water must be considered for future application, as the observed maximum pot-life of the NCO component in an aqueous solution was found to be 10 min. Therefore, supply of the pure NCO component and dilution with water shortly before application are required. Regular discussions with surgeons confirmed that a time frame of 10 min is sufficient for application of the hydrogel components during surgery.

The overall concentration of the NCO component in the presented hydrogel system after addition of the NH_2 component is set to 10 wt %, which is equivalent to a concentration of 0.255 wt % of pure NCO groups. Assuming a conversion of 75% NCO during the first seconds, as visible from Figure 2, 0.064 wt % of NCO groups would remain in the hydrogel system for an additional 92 min, being equal to 0.024 g of NCO groups. This amount might not strongly influence the biocompatibility, as it is bound to a macromolecular backbone, which is reported to reduce toxicity effects in comparison to isocyanate monomers.[22]

Rheological Determination of Viscoelastic Properties. Because rheology is a sensitive method to detect changes in a polymer structure or in a formulation, in the following, rheology was used as a fast and accurate method to characterize the hydrogel formulation.

The results of the dynamic oscillation tests depicted in Figure 3A demonstrate that the end of the linear viscoelastic region (LVER) of the analyzed PUU hydrogel is reached at a shear strain of approximately $\gamma = 10\%$ because, above that value, the loss modulus G'' starts to increase. This can be explained by the formation of microcracks at higher deformations causing a higher degree of internal friction. The relative standard deviation (RSD) within the LVER is

https://doi.org/10.1021/acsomega.4c04577
ACS Omega 2024, 9, 34008−34020

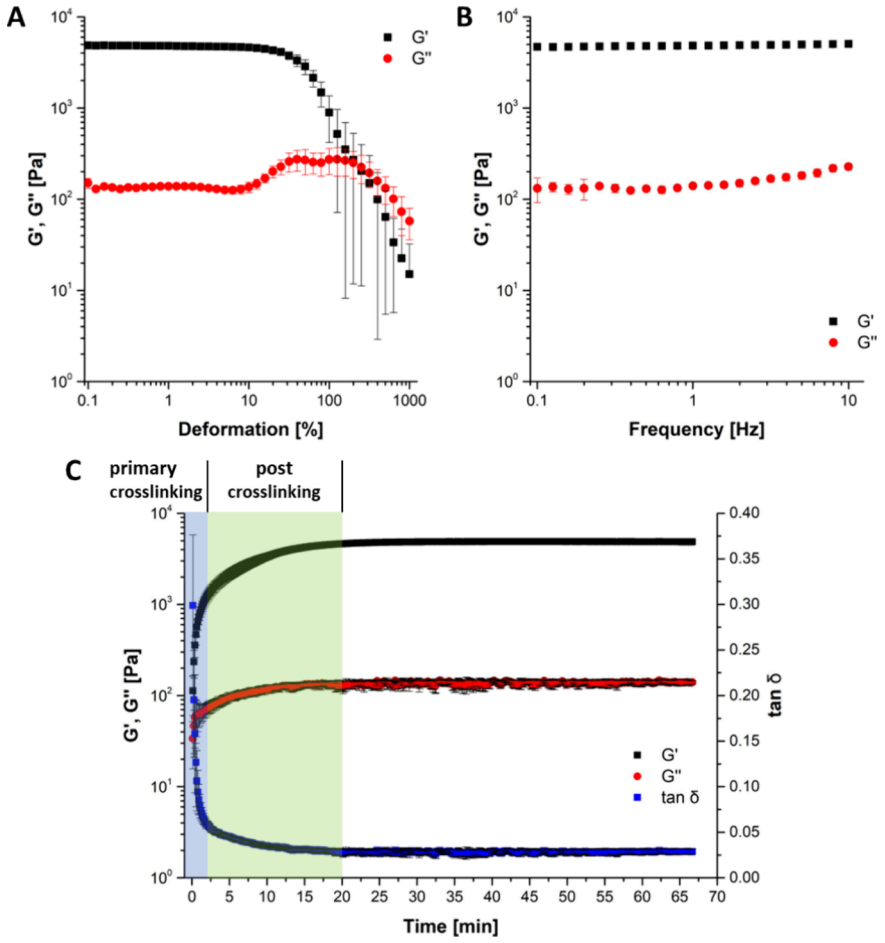

Figure 3. Rheological characterization of the reported PUU hydrogel. (A) Amplitude sweeps of the cured hydrogel at a constant frequency (1 Hz) with increasing shear strains (0.1 to 1000%) were conducted to determine the viscoelastic properties of the PUU hydrogel, in particular the storage modulus G' and loss modulus G'' as a function of time. (B) Frequency sweeps of the cured hydrogel at a constant shear strain (γ = 1%) and decreasing frequencies from 10 to 0.1 Hz. G' and G'' are presented as a function of frequency. (C) Time sweep using parameters within the linear viscoelastic region determined in previous tests (f = 1 Hz, γ = 1%). Data are presented as G', G'', and loss factor tan δ as a function of time. All analyses were performed in triplicate. Error bars: SD.

remarkably low (G' < 8%; G'' < 12%), whereas RSDs increase after leaving the LVER due to nonreproducible destruction of the structure and unavoidable normal forces of the viscoelastic substance that lead to an edge failure.[23] As demonstrated in the tensile test, which is discussed at a later stage, the microcracks do not influence the applicability of the hydrogel, and requirements regarding the elongations are still met.

Frequency sweeps enable the analysis of the material frequency dependence. Figure 3B clearly shows the formation of a three-dimensional polymer network because G' and G'' occurred as parallel functions over the entire frequency range with $G' > G''$. A potential change from solid to liquid behavior of the hydrogel inside the abdomen due to deformation caused by organ movements in different frequencies can therefore be excluded.

Based on the results from the amplitude sweep and frequency sweep, an appropriate frequency and amplitude were selected for performing a time sweep, by which the gelation behavior of the hydrogel was analyzed. In surgery, a curing time <60 s is regarded as desirable. The time-dependent behavior of the hydrogel starting with the initial mixing of both components can be found in Figure 3C, revealing that the point of gelation ($G' = G''$) was reached before the first measuring point was recorded. Hence, the transition from liquid-like to solid-like behavior during the gelation process is reached rapidly (<8 s). The curing time is therefore clearly below the targeted 60 s, and gelation is comparable or even superior to different *in situ* gelling systems that have been previously established in surgery such as SprayShield or BioGlue.[24,25] RSDs of up to 53% for both moduli were observed during the first minute of gelation, which can be explained by a nonreproducible mixing of both components on the plate or slightly varying time lags between mixing and start of the measurements. However, high RSDs during rheological characterizations are commonly observed.[26] The gelation process is finished after approximately 20 min, when G', G'', and loss factor tan δ reach a plateau (G' ~4900 Pa; G'' ~140 Pa; tan δ ~0.03). The extremely low tan δ highlights the almost ideally elastic behavior of the hydrogel because G' completely dominates G''. Based on the results of the time sweep, the gelation process can be divided in two main phases: primary cross-linking and post cross-linking. Primary cross-linking is defined by the rapid cross-linking process of NCO and NH_2 groups, resulting in a stable three-dimensional network that is revealed by a rapid increase of G' and a decrease of tan δ, respectively. The first phase is complete after approximately 3 min. This phase is subsequently followed by the post cross-linking process with a much slower gelation rate,

https://doi.org/10.1021/acsomega.4c04577
ACS Omega 2024, 9, 34008−34020

which terminates after ∼20 min. Post cross-linking is the phase where the majority of NCO and NH_2 groups have reacted so that a stable three-dimensional network has already been established. However, here the gelation is still in progress, but the reaction rate has slowed down, as is judged by less rapidly changing values for G', G'', and tan δ. The transition between these two phases was defined as the inflection point at which the slope of tan δ is flattening.

Therefore, the herein reported rheological measurements and results represent a valuable base for executing a rheological validation process.[23,26]

pH Values of Resulting Hydrogels. Because the hydrogel presented herein is applied as a 2K system comprising an amine curing component, the curing reaction is investigated in detail with regard to physiological pH values. HCl is added to the formulation as a buffering agent in a defined amount to ensure pH values of the hydrogel in a physiological range of ≤7.4.[27]

pH values measured as a function of the time of the hydrogel curing process are depicted in Figure 4. Additionally, crucial values are presented in Table 1, namely, the highest pH value, the time until the highest measured pH-value is reached, the time until the pH drops below pH 7.4 (indicating biocompatibility), and the pH value after 30 min. As visible from Table 1, the alkaline peak of pH is reached after 9 ± 5 s at 8.31 ± 0.22, leading to physiological pH values (≤7.4) after 76 ± 36 s.

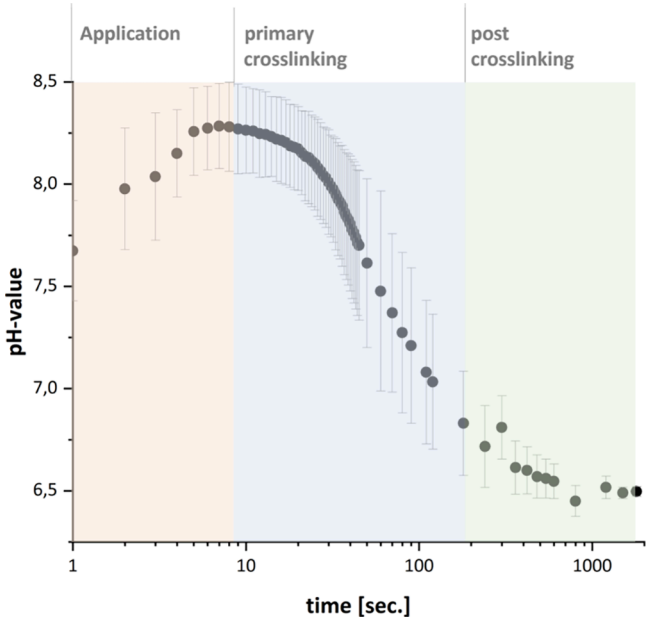

Figure 4. pH curve of the cross-linking reaction of the herein reported 2K hydrogel system as mean values (n = 3) with SD as error bars. The alkalic peak of the pH value was reached within 9 s with an average of 8.31 ± 0.22. The time at which the pH falls below 7.4 was found to be 76 ± 36 s. After 30 min, the pH reached a value of 6.5 ± 0.02. A proposed three-stage process of cross-linking reaction is marked in different colors. (1) Application: Herein, both solutions are applied, which results in a visible increase of pH due to increased NH_2 concentration. (2) Primary cross-linking: initial cross-linking process of NH_2 and NCO groups, visible as a rapid decrease in pH values. (3) Post cross-linking: pH decrease is still present but less rapid than in primary cross-linking, indicating that the cross-linking process is still ongoing.

Table 1. Summary of Resulting pH Values of the PUU Hydrogel Giving the Highest Measured pH Value, the Time When It Was Measured, the Time at which pH Is Equal or Decreased to 7.4 as Indicator for Biocompatibility, and the Resulting pH Value after 30 min (n = 3)

pH_{max}	t (pH_{max}) [s]	t (pH ≤ 7.4) [s]	pH (t = 30 min)
8.31 ± 0.22	9 ± 5	76 ± 36	6.50 ± 0.02

The initial maximum pH was found to be 8.31, and physiological values (≤7.4) were reached after 76 s. Although alkaline conditions above pH 7.4 are known to support bacterial growth and pH values in chronic wounds were described to range from 7.42 to 8.90, it is unlikely that short-term exposure for 76 s poses comparable risks. Whereas deviations to higher values can support the presence of chronic wounds, deviations to lower pH values are described to support the wound healing process by their slightly acidic milieu, as the pH value strongly influences relevant enzyme activities.[28,29] Clinical indicators of lower pH milieu in wounds (≤6.1 ± 0.6 SD) comprise pus, necrotic tissue, and serum crusts.[29] Hence, a pH range between 6.1 and 7.4 is not expected to interfere with the sensitive wound healing processes. Our herein presented PUU hydrogel fulfills this requirement.

As visualized by the different colored areas in Figure 4, the resulting pH curve can be divided into three different stages: application, primary cross-linking, and post cross-linking. Application is defined as the initial mixing step, where single reactants are mixed with each other. This stage is characterized by a rapid increase of the pH values caused by the diffusion of the amine-containing reaction mixtures into the pH electrode. The second stage, primary cross-linking, is defined as rapid cross-linking of NCO and NH_2 groups, which can be traced by a strong decrease in pH that corresponds to the conversion of NH_2 to urea cross-links. The onset of the final stage of post cross-linking can be defined as the point after which the majority of NH_2 and NCO groups have cross-linked. However, gelation is still proceeding at a lower reaction rate, and hence, the pH decreases less rapidly. Considering the reaction kinetics of primary amines with isocyanates, a fast and complete conversion of all amine groups is expected.[30] The post cross-linking process could probably be a result of delayed curing due to a rigidification of the network. However, with increasing network density, the mobility of functional groups decreases. Additionally, as the reaction proceeds, the isocyanate-amine reaction might start to compete with the hydrolysis of isocyanates to yield amines that react with residual isocyanate groups in close proximity. Further decrease of pH values could be a result of eliminated CO_2 during the reaction of NCO with H_2O.

During the stage of application, the pH rises until 8.31 ± 0.22 after 9 ± 5 s caused by the increased concentration of amine on the surface of the electrode, induced by applying single solutions of NCO and NH_2 into the beaker. A pH of 7.4 is reached after 76 ± 36 s. After 20 min, only minor changes were detected (6.52 to 6.49, n = 3). Thus, after 30 min, the pH value of the hydrogel appears to be stable.

Rheological measurements (Figure 3) support the theory of the three consecutive stages during hydrogel formation (application, primary cross-linking, and post cross-linking). However, the stage of application is not detectable in rheological measurements caused by a time lag between

https://doi.org/10.1021/acsomega.4c04577
ACS Omega 2024, 9, 34008−34020

mixing and the start of the measurements. The detected times of transition in both measurements (pH and rheology) are comparable. We have defined transitions from application to primary cross-linking to post cross-linking by the respective inflection points of the curves of pH and rheological measurements, hypothesizing that both measurements depict the same process. After 20 min, no major alterations have been detected in both measurements.

Mechanical Properties. Apart from common body movements, larger mechanical forces within the abdominal area might arise from coughing, sneezing, or physiological movement.[31] To investigate whether the herein presented hydrogels are able to withstand such forces, tensile tests have been conducted on four samples, prepared as an S-2 test specimen (dog-bone), to determine the elongation at break and tensile strength at break.

Results of average values (n = 4) of the PUU hydrogel are presented in Figure 5. As illustrated, all samples prepared for

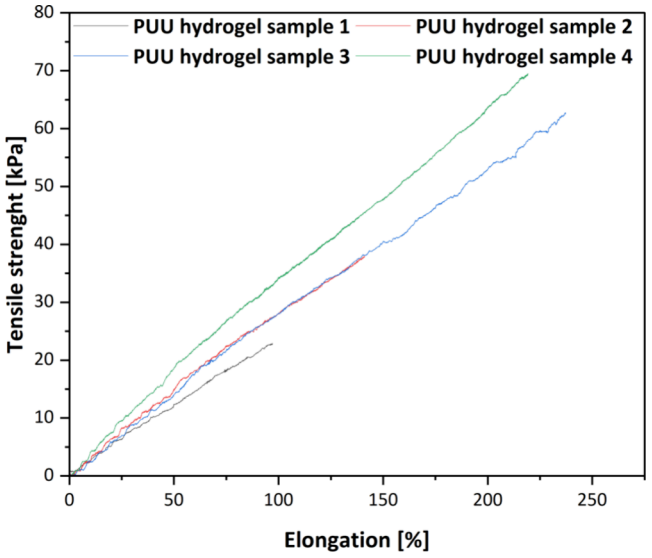

Figure 5. Fourfold tensile testing of PUU hydrogel samples 1−4 with reached elongations of 99−237% and reached tensile strengths of 23−69 kPa.

tensile tests comprise elongations from 99 to 237% with an average of 174.3 ± 65.1%. Deviations are presumably caused by small fractures during sample preparation. Tensile strength at break was measured between 23 and 69 kPa with an average of 48.2 ± 21.6 kPa.

All samples of the fourfold measurements revealed at least an elongation of 99% (mean = 174.3 ± 65.1%). This underlines the hydrogels' suitability for an application on the abdominal wall, as Junge et al. reported mean elongations of only 11 to 32% of human tissue taken from the abdominal wall *post mortem* when applying a strain of 16 N.[32] Although these experiments are restricted in their comparability to elongations occurring *in vivo*, they at least provide a hint of the distensions to be expected. Thus, the expansibility of the PUU hydrogel can be considered sufficient for application on the abdominal wall.

Tensile strength at break of single samples varied between 23 and 69 kPa (mean = 48.2 ± 21.6 kPa) in the fourfold measurements conducted.

Hydrolytic Degradation. The aim of the hydrogel is to form a stable adhesion barrier for at least 7 days because fibroblasts predominate 5 to 7 days after surgery. This means that adhesions can only be formed within the first 7 days after surgery.[13,33]

The degradation process of the hydrogel is based on hydrolytic cleavage of the lactide within the polymer structure and was monitored by analyzing the weight loss after drying using gravimetrical analysis (Figure 6A). The degradation products were analyzed in terms of concentration, molecular weight, and dispersity $Đ_M$ via gel permeation chromatography (GPC). As seen in Figure 6B, two main fractions of the degradation products were present. The minor fraction (fraction 1) appeared in low concentrations between 0.14 ± 0.08 (0 day) and 1.0 ± 0.4 mg mL^{-1} (21 days), whereas concentrations between 1.9 ± 0.9 (0 day) and 10.8 ± 1.5 mg mL^{-1} (14 days) were observed for the major fraction (fraction 2). These results demonstrate that the gravimetrical and GPC analyses were in good agreement because the total concentration of both fractions corresponded to the gravimetrically determined weight loss of the hydrogels. Figure 6C visualizes that the molecular weights in fraction 1 increased from 717,000 ± 74,000 (0 day) to 1,462,000 ± 370,000 g mol^{-1} (21 days), whereas fraction 2 contains significantly smaller molecules, with molecular weights increasing from 29,000 ± 4800 (0 day) to 48,000 ± 7400 g mol^{-1} (21 days). A reason for the increasing molecular weight in the fractions over time might be that, initially, only superficial degradation occurs by terminal polymer chain cleavage. Over time, larger oligomers located deeper within the hydrogel are also cleaved off. The resulting increase of the molecular weight can then indicate the presence of these larger molecules in solution. Moreover, as large oligomers of fraction 1 become further cleaved over time, they contribute to an increased molecular weight of fraction 2.

Additionally, the degradation products displayed dispersities within 1.9 ± 0.7−2.6 ± 0.5 (fraction 1) and 2.2 ± 0.1−3.4 ± 0.3 (fraction 2), respectively (Figure 6D). Interestingly, a trend toward higher dispersities can be noticed for fraction 1, whereas the dispersity for fraction 2 tends to decrease with time. The increasing dispersity of fraction 1 is related to the above-mentioned explanation, as the dispersity increased as larger molecules became released into the supernatant. The reduction of the dispersity in fraction 2 however was a result of a proceeding cleavage of the smaller fragments, which resulted in a convergence of the degradation products to a smaller size.

Thus, the results from the degradation study revealed that full degradation was observed after only 14 days, which is sufficient to prevent the formation of adhesions.

A crucial parameter for a suitable biodegradable hydrogel to consider is the maximum size of a molecule that can be eliminated by the body. Renal elimination of molecules up to 50,000 g mol^{-1} is unproblematic, whereas molecules with molecular weights similar to albumin or higher (67,000 g mol^{-1}) damage the glomerular filtration barrier.[34,35] Because fraction 2 exhibited a maximum molecular weight of 48,000 g mol^{-1}, a renal excretion with regard to this fraction is feasible. Furthermore, the renal elimination of fraction 1 is possible over time because a follow-up study of three independent hydrogel samples after 11 months demonstrated a complete cleavage of the hydrogel. In this case, only one fraction could be observed, with molecular weights low enough to be renally eliminated (M_W = 23,800 ± 3300 g mol^{-1}, $Đ_M$ = 1.8 ± 0.2).

https://doi.org/10.1021/acsomega.4c04577
ACS Omega 2024, 9, 34008−34020

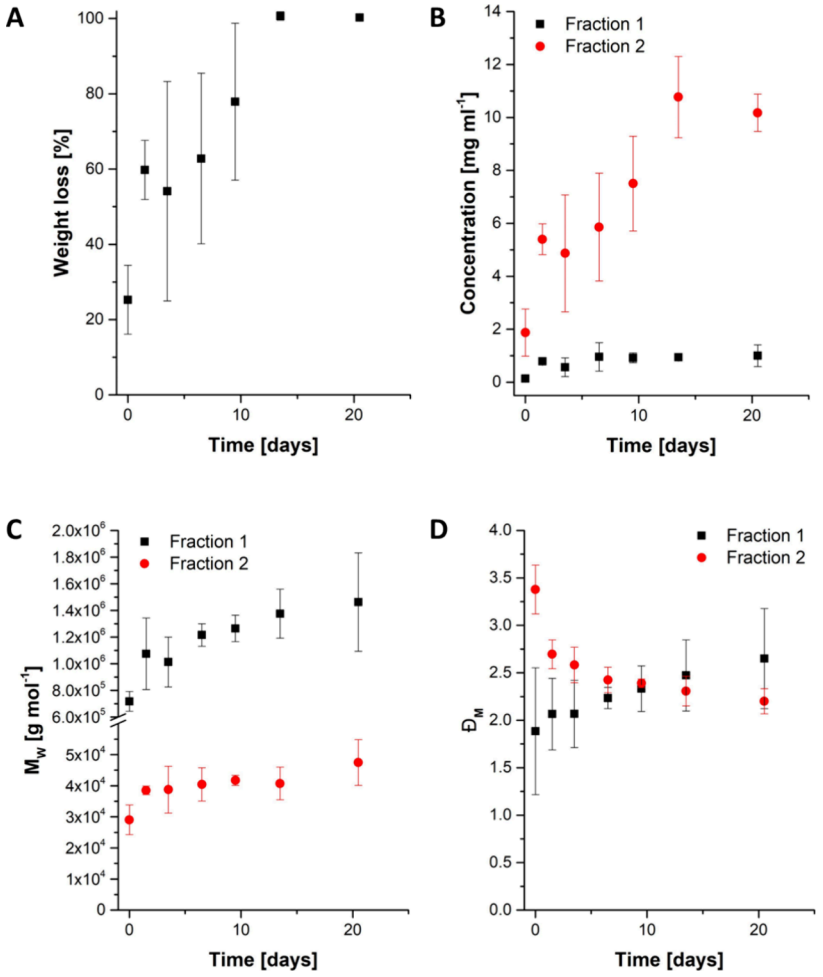

Figure 6. Hydrolytic degradation studies of the PUU hydrogel in DPBS. (A) Weight loss of hydrogels in DPBS buffer (1×) at 37 °C. (B) Concentration of degradation products in the supernatant. (C) Molecular weight M_W of degradation products in the supernatant. (D) Dispersity $Đ_M$ of degradation products in the supernatant. Data were obtained from three independent experiments. Error bars: SD.

Importantly, tuning of the degradation rate would be feasible by a modification of the lactide content within the prepolymer. A higher content of lactide functionalities would result in faster degradation along with smaller decomposition products.

Pyrogen Testing. Preliminary tests (data not shown) revealed that investigating the hydrogel in terms of endotoxins using a LAL test was not feasible because acceptance criteria for the recovery of spiked endotoxins (between 50 and 200%) could not be met. Possible reasons could either be a masking effect or an adsorption effect of endotoxins onto the hydrogel leading to a depletion of the endotoxins from the supernatant, which was the specimen assayed in the LAL test. Hence, a monocyte activation test (MAT) was conducted as an alternative to detect possible endotoxins present in the hydrogel. Here, the monocytic cells were directly added to the incubated hydrogel, meaning that the cells are in direct contact to the solid material and not only to the extracted compounds that are present in the supernatant. The MAT demonstrated the absence of endotoxins in the hydrogel with an endotoxin content below the lower limit of quantification (<0.05 EU mL^{-1}).

Absence of Cytotoxic and Mutagenic Effects of PUU Hydrogel Degradation Products. Adhesion prevention requires the hydrogel to serve as a barrier for migrating cells while not negatively affecting the viability of the surrounding tissue. Therefore, to rule out any detrimental effects of gel degradation products, cytotoxicity and mutagenicity testing was performed. The cytotoxicity of the degradation products was assessed using an assay for metabolic activity (MTT assay), which was conducted by testing varying concentrations of PUU gel extracts (undiluted, 1:2, 1:5, 1:10). Two different incubation time periods to obtain gel extracts were chosen to investigate cytotoxicity during the critical period of wound healing and at the end of the degradation process (Figure 7) to exclude the cytotoxicity of smaller molecules that were formed during degradation (14 days). According to ISO 10993-5, the cytotoxicity threshold was set to <70% viability of the negative control condition. Relative to cell viability in the culture medium, which was defined as 100%, no cytotoxic effects of any PUU gel extracts on A549 cells were observed.

An HPRT assay was conducted to exclude mutagenic effects of day 7 PUU hydrogel degradation products. CHO-K1 cells treated with the mutagenic control substances ethyl methanesulfonate and benzo[*a*]pyrene formed >50 colonies after selection with 6-thioguanine, indicative of mutations in the *HPRT* gene. The number of colonies increased with increasing concentration of the mutagenic agent. Cells treated with degradation extracts of varying concentrations (undiluted, 1:2, 1:5, 1:10) with or without metabolic activation formed <15

https://doi.org/10.1021/acsomega.4c04577
ACS Omega 2024, 9, 34008−34020

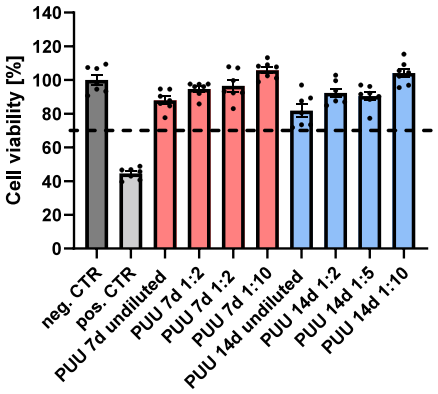

Figure 7. Cytotoxicity testing of the PUU hydrogel extracts. The cytotoxicity of PUU hydrogel extracts was assessed using an MTT assay. A cytotoxic effect was defined as <70% viability of the negative control (neg. CTR, i.e., culture medium). pos. CTR = staurosporine (10 μM). Data points represent values obtained from individual wells. Error bars: SEM.

colonies after selection. Therefore, we concluded that the extracts did not induce significant mutagenic effects (Figure 8).

PUU Hydrogels Reduce Surface Cell Adhesion and Form a Barrier for Migrating Cells. To test its function as a barrier for adhesion prevention, PUU hydrogels that were in direct contact with cells were studied. First, A549 cells were seeded on polymerized PUU hydrogels to study how well cells can adhere to the gel surface. Forty-eight hours after cell seeding, significantly fewer adherent cells were observed on PUU hydrogels compared to Matrigel (Figure 9A,B). Additionally, the percentage of the gel surface covered with cells was also significantly lower (Figure 9C).

Next, we aimed to investigate whether the remaining proportion of cells adhering to the PUU hydrogel surface would be able to invade the gel or migrate through it. To address this question, we cultured cells on the gel surface, stimulated cell invasion using a serum gradient, and quantified the number of invasive cells that transversed the gel and the underlying porous membrane after 7 days. At this time point, a significantly larger number of invasive cells were observed in Matrigel compared to PUU hydrogels (Figure 10A,B), which was reflected in a statistically significant reduction of the percentage of the PUU gel surface covered with cells (Figure 10C).

Overall, the PUU hydrogels showed low levels of surface cell adhesion and invasion, supporting their function as cellular barriers for adhesion prevention during the critical period of wound healing after surgery. Cell surface adhesion to hydrogels is mostly mediated by absorption of proteins by the gel surface, which enables cell binding via, e.g., integrin receptors.[36] A possible explanation for the antiadhesive properties of the PUU hydrogels could be a surface layer of water molecules binding to the hydrogel PEG units via hydrogen bonds.[37] This layer of water molecules might reduce the absorption of proteins and therefore cell attachment, as it has been proposed by other studies using polyurethan-based and natural polysaccharide-based hydrogels.[38,39]

In line with the low cell adhesion, we also observed that PUU hydrogels prevented excess cell invasion. Previously, a similar assay, using a serum gradient to stimulate cell invasion in a Transwell-system, was employed by Chou and colleagues to study cell invasion in poly-*N*-isopropylacrylamide-based

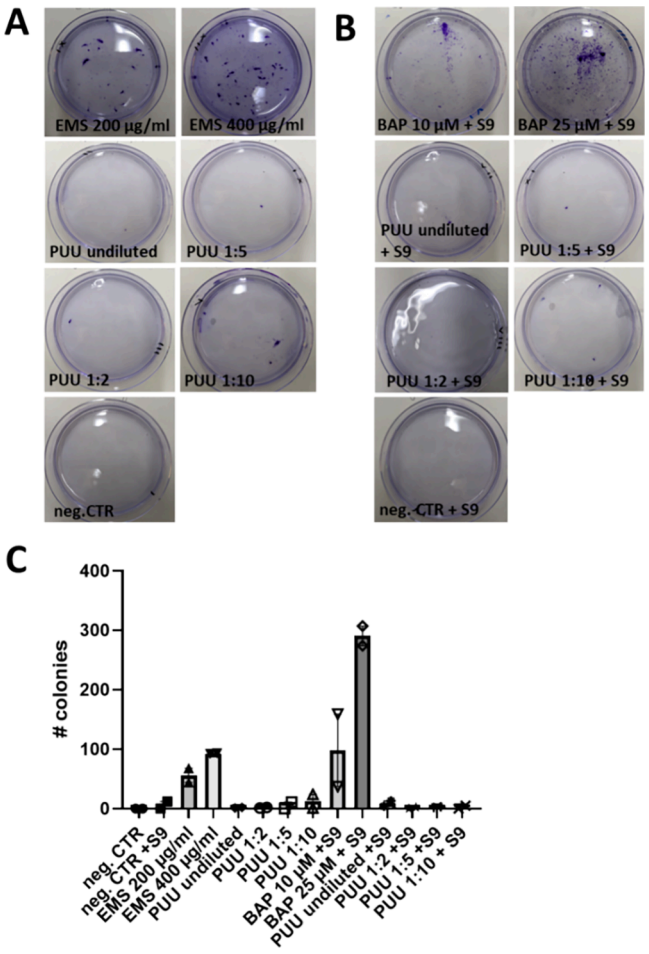

Figure 8. Mutagenicity testing of the PUU hydrogel extracts. An HPRT assay was performed to exclude mutagenic effects of PUU hydrogel extracts. (A) Photographs of Petri dishes with crystal violet-stained colonies after selection with 6-thioguanine (treatment conditions without exogenous metabolic activation, EMS = ethyl methanesulfonate, neg. CTR = culture medium). (B) Photographs of Petri dishes with crystal violet-stained colonies after selection with 6-thioguanine (treatment conditions with exogenous metabolic activation, BAP = benzo[*a*]pyrene, neg. CTR = culture medium). (C) Quantification of colonies with a minimum size of 10 cells. Data points represent values obtained from individual Petri dishes. Error bars: SEM.

hydrogels.[40] Besides the initially low attachment of cells, which reduces the number of possible invading cells, there are several factors that can influence cell penetration. These include gel stiffness, cross-linking density (mesh size), and network structure of the hydrogels.[41] As suggested by our degradation data, cleavage of lactide units was already in progress at the time point tested. However, PUU gels maintained their barrier function until this critical time point, suggesting that they are suitable materials for adhesion prevention.

CONCLUSIONS

Overall, we describe a novel 2K sprayable adhesion barrier that can be applied in minimally invasive surgery. The hydrogel reported herein combines the advantages of sprayability, biodegradability, rapid curing, and shape adaption. We demonstrate antiadhesive and antiinvasive properties of the PUU hydrogels, confirming that the gels provide a suitable barrier to prevent or minimize the formation of postoperative

https://doi.org/10.1021/acsomega.4c04577
ACS Omega 2024, 9, 34008−34020

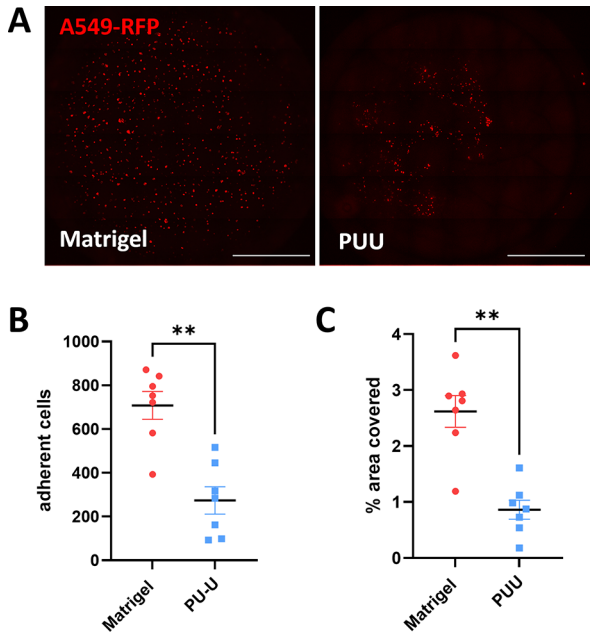

Figure 9. Cell adhesion on the hydrogel surface 48 h after seeding. (A) Representative images of RFP-positive adherent A549 cells 48 h after seeding on the surface of Matrigel and PUU hydrogels. Scale bars: 1 mm. (B) Total count of adherent cells (Mann−Whitney test, p = 0.0041**). (C) Percentage of gel surface covered with cells (Mann−Whitney test, p = 0.0012**). Error bars: SEM.

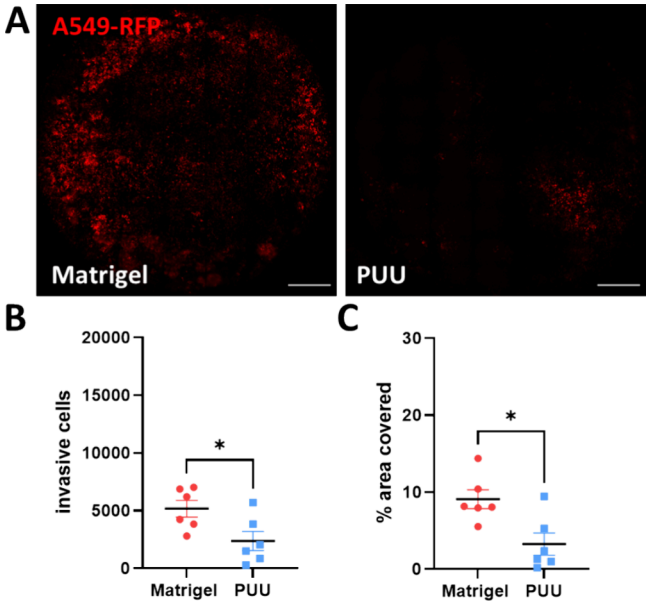

Figure 10. Cell invasion into hydrogels. (A) Representative images of RFP-positive A549 cells adherent to the Thincert membrane after transversion of Matrigel and PUU hydrogels for 7 days. Scale bars: 1 mm. (B) Quantification of invasive cells after 7 days (Mann−Whitney test, p = 0.026*). (C) Percentages of the Thincert membrane covered with cells after 7 days (Mann−Whitney test, p = 0.026*). Error bars: SEM.

adhesions. At the same time, we examined the kinetics of the degradation process and additionally show that degradation products of the gels are noncytotoxic and do not elicit mutagenic effects, which is critically important for future usage of the gels in *in vivo* studies. Regarding potential toxicological harm using an NCO-based prepolymer, we showed that full NCO conversion is reached after 92 min, while 75% of NCO groups were instantly converted at the beginning of the reaction, indicating a reduced risk of toxicological harm. Analysis of the pH values during the curing reaction of the hydrogel revealed that the use of NH_2 terminated cross-linker initially leads to an increase in pH values. However, hydrogels exhibit physiological pH values 76 s after application. If the alkaline pH stage in the beginning of the cross-linking process is critical, this needs to be further investigated in advanced biocompatibility tests. There are some limitations of our study that should be addressed in future experiments. The lung cancer cell line A549, which was used in this study, is routinely used for studies of cell invasion in the literature and shows enhanced migratory capacity during epithelial−mesenchymal transition (EMT).[42] Nevertheless, it would be important to assess the hydrogel barrier function using more relevant cells, for example, primary peritoneal fibroblasts or mesothelial cells. Ultimately, *in vivo* spray application of PUU hydrogels should be performed to investigate the barrier function after surgery in a physiological system in which a mixture of tissue-resident cells and immune cells is present.

■ ASSOCIATED CONTENT

Supporting Information

The Supporting Information is available free of charge at https://pubs.acs.org/doi/10.1021/acsomega.4c04577.

Polyol synthesis, prepolymer synthesis, $^{1}H/^{13}C$ NMR spectra, FTIR spectra, and dilution ratios for HPRT assay (PDF)

■ AUTHOR INFORMATION

Corresponding Author

Tobias Hokamp − *NMI Natural and Medical Sciences Institute at the University of Tübingen, Reutlingen 72770, Germany; NMI Technology Transfer GmbH, Reutlingen 72770, Germany;* orcid.org/0009-0004-3280-2662; Email: Tobias.Hokamp@nmi.de

Authors

Lana Kortenbrede − *Covestro Deutschland AG, Coatings and Adhesives, Leverkusen 51365, Germany*

Johanna Heider − *NMI Natural and Medical Sciences Institute at the University of Tübingen, Reutlingen 72770, Germany*

Heike Heckroth − *Covestro Deutschland AG, Coatings and Adhesives, Leverkusen 51365, Germany*

Marc Leimenstoll − *Macromolecular Chemistry, Cologne University of Applied Science, Leverkusen 51379, Germany*

Heiko Steuer − *NMI Technology Transfer GmbH, Reutlingen 72770, Germany*

Jan Sütterlin − *Covestro Deutschland AG, Coatings and Adhesives, Leverkusen 51365, Germany*

Frank Weise − *NMI Natural and Medical Sciences Institute at the University of Tübingen, Reutlingen 72770, Germany*

Complete contact information is available at: https://pubs.acs.org/10.1021/acsomega.4c04577

Author Contributions

[⊥]L.K. and J.H. contributed equally. The manuscript was written through contributions of all authors. J.H., L.K., and T.H. developed and conducted the experiments. All authors have given approval to the final version of the manuscript.

Funding

Financial support was provided by the Federal Ministry of Education and Research (funding codes: 13XP5107A and13XP5107C)

Notes

The authors declare no competing financial interest.

■ ACKNOWLEDGMENTS

We greatly acknowledge Dr. Thomas Joos for his technical supervision during the whole project. Additionally, we would like to thank Prof. Dr. Axel G. Griesbeck, from the University of Cologne, for continuous technical support and constant efforts. We thank Jun. Prof. Dr. med. Martin Weiss for continuous helpful discussions and feedback. Additionally, we acknowledge Erbe Elektromedizin, especially Dr. Sascha Dammeier, Frank Straub, and Andreas Fech, for continuous technical and practical support. We would like to thank Ina Beck for technical support. Funding was provided by the Federal Ministry of Education and Research (funding codes: 13XP5107A and13XP5107C). Graphical abstract was created with Biorender.com.

■ ABBREVIATIONS

HA, hyaluronic acid; CMC, carboxymethyl cellulose; PLA, polylactic acid; ePTFE, expanded polytetrafluorethylene; PUU, polyurethane urea; 2K, two component; NCO, isocyanate; NH_2, primary amine; EO, ethylene oxide; *f*, functionality; HCl, hydrochloric acid; LVER, linear viscoelastic region; HPRT, hypoxanthine−guanine phosphoribosyltransferase; RSD, relative standard deviation; SD, standard deviation; G'', loss modulus; G', storage modulus; tan δ, loss factor; GPC, gel permeation chromatography; DPBS, deionized phosphate buffered saline; LAL, limulus amoebocyte lysate; FCS, fetal calf serum; MAT, monocyte activation test; MTT, assay metabolic activity assay; CTR, control; EMS, ethyl methanesulfonate; BAP, benzo[*a*]pyrene; SEM, standard deviation of mean; PEG, polyethylene glycol; EMT, epithelial−mesenchymal transition.

■ REFERENCES

(1) Mantha, S.; Pillai, S.; Khayambashi, P.; Upadhyay, A.; Zhang, Y.; Tao, O.; Pham, H. M.; Tran, S. D. Smart Hydrogels in Tissue Engineering and Regenerative Medicine. *Materials* **2019**, *12* (20), 3323.

(2) Huang, C.; Dong, L.; Zhao, B.; Lu, Y.; Huang, S.; Yuan, Z.; Luo, G.; Xu, Y.; Qian, W. Anti-inflammatory hydrogel dressings and skin wound healing. *Clin. Transl. Med.* **2022**, *12* (11), No. e1094.

(3) Haworth, K.; Travis, D.; Abariga, S. A.; Fuller, D.; Pucker, A. D. Silicone hydrogel versus hydrogel soft contact lenses for differences in patient-reported eye comfort and safety. *Cochrane Database Syst. Rev.* **2021**, CD014791.

(4) Vigata, M.; Meinert, C.; Hutmacher, D. W.; Bock, N. Hydrogels as Drug Delivery Systems: A Review of Current Characterization and Evaluation Techniques. *Pharmaceutics* **2020**, *12* (12), 1188.

(5) Cai, J.; Guo, J.; Wang, S. Application of Polymer Hydrogels in the Prevention of Postoperative Adhesion: A Review. *Gels* **2023**, *9* (2), 98.

(6) Choudhary, B.; Paul, S. R.; Nayak, S. K.; Qureshi, D.; Pal, K. Synthesis and biomedical applications of filled hydrogels. In *Polymeric Gels*; Elsevier, 2018; pp 283−302. DOI: .

(7) Wichterle, O.; Lím, D. Hydrophilic Gels for Biological Use. *Nature* **1960**, *185* (4706), 117−118.

(8) Aswathy, S. H.; Narendrakumar, U.; Manjubala, I. Commercial hydrogels for biomedical applications. *Heliyon* **2020**, *6* (4), No. e03719. Published Online: Apr. 7, 2020.

(9) Lauder, C. I. W.; Garcea, G.; Strickland, A.; Maddern, G. J. Abdominal adhesion prevention: still a sticky subject. *Dig. Surg.* **2010**, *27* (5), 347−358. Published Online: Sep. 16, 2010.

(10) Vrijland, W. W.; Jeekel, J.; Van Geldorp, H. J.; Swank, D. J.; Bonjer, H. J. Abdominal adhesions: intestinal obstruction, pain, and infertility. *Surg. Endosc.* **2003**, *17* (7), 1017−1022. Published Online: Mar. 14, 2003.

(11) Weibel, M. A.; Majno, G. Peritoneal adhesions and their relation to abdominal surgery. A postmortem study. *Am. J. Surg.* **1973**, *126* (3), 345−353.

(12) Park, H.; Baek, S.; Kang, H.; Lee, D. Biomaterials to Prevent Post-Operative Adhesion. *Materials* **2020**, *13* (14), 3056.

(13) Boland, G. M.; Weigel, R. J. Formation and prevention of postoperative abdominal adhesions. *J. Surg. Res.* **2006**, *132* (1), 3−12. Published Online: Feb. 2, 2006.

(14) Fatehi Hassanabad, A.; Zarzycki, A. N.; Jeon, K.; Dundas, J. A.; Vasanthan, V.; Deniset, J. F.; Fedak, P. W. M. Prevention of Post-Operative Adhesions: A Comprehensive Review of Present and Emerging Strategies. *Biomolecules* **2021**, *11* (7), 1027.

(15) Ahmad, M.; Crescenti, F. Significant Adhesion Reduction with 4DryField PH after Release of Adhesive Small Bowel Obstruction. *Surg. J.* **2019**, *5* (1), e28−e34. Published Online: May. 10, 2019.

(16) Rastan, A.; Mohr, F. W.; Rastan, A. J. Bioresorbable adhesion barrier for reducing the severity of postoperative cardiac adhesions: Focus on REPEL-CV(®). *Med. Devices: Evidence Res.* **2011**, *4*, 17−25. Published Online: Jan. 12, 2011.

(17) Haney, A. F.; Doty, E. A barrier composed of chemically cross-linked hyaluronic acid (Incert) reduces postoperative adhesion formation. *Fertil. Steril.* **1998**, *70* (1), 145−151.

(18) Wallwiener, M.; Brucker, S.; Hierlemann, H.; Brochhausen, C.; Solomayer, E.; Wallwiener, C. Innovative barriers for peritoneal adhesion prevention: liquid or solid? A rat uterine horn model. *Fertil. Steril.* **2006**, *86* (4 Suppl), 1266−1276.

(19) Kortenbrede, L.; Heckroth, H.; Sütterlin, J. *Method of manufacturing a hydrogel useful for preventing post-surgical adhesions*. PCT/EP2023/085794.

(20) Stockmayer, W. H. Molecular distribution in condensation polymers. *J. Polym. Sci.* **1952**, *9* (1), 69−71.

(21) Delebecq, E.; Pascault, J. P.; Boutevin, B.; Ganachaud, F. On the Versatility of Urethane/Urea Bonds: Reversibility, Blocked Isocyanate, and Non-isocyanate Polyurethane. *Chem. Rev.* **2013**, *113* (1), 80−118.

(22) Fernando, S.; McEnery, M.; Guelcher, S. A. Polyurethanes for bone tissue engineering. In *Advances in Polyurethane Biomaterials*; Elsevier, 2016; pp 481−501. DOI: .

(23) Mezger, T. G. *The rheology handbook:For users of rotational and oscillatory rheometers*, Fifth revised ed.; Vincentz Network, 2020.

(24) Banasiewicz, T.; Horbacka, K.; Karoń, J.; Malinger, S.; Antos, F.; Rudzki, S.; Kala, Z.; Stojcev, Z.; Kössi, J.; Krokowicz, P. Preliminary study with SprayShield Adhesion Barrier System in the prevention of abdominal adhesions. *Wideochirurgia i inne techniki maloinwazyjne = Videosurgery and other miniinvasive techniques* **2013**, *8* (4), 301−309. Published Online: May. 6, 2013.

(25) Chao, H. H.; Torchiana, D. F. BioGlue: albumin/glutaraldehyde sealant in cardiac surgery. *J. Card. Surg.* **2003**, *18* (6), 500−503.

(26) Simões, A.; Miranda, M.; Cardoso, C.; Veiga, F.; Vitorino, C. Rheology by Design: A Regulatory Tutorial for Analytical Method Validation. *Pharmaceutics* **2020**, *12* (9), 820.

(27) Hopkins, E.; Sanvictores, T.; Sharma, S. *Physiology, Acid Base Balance*; StatPearls, 2024.

(28) Power, G.; Moore, Z.; O'Connor, T. Measurement of pH, exudate composition and temperature in wound healing: a systematic review. *J. Wound Care* **2017**, *26* (7), 381−397.

(29) Schneider, L. A.; Korber, A.; Grabbe, S.; Dissemond, J. Influence of pH on wound-healing: a new perspective for wound-

https://doi.org/10.1021/acsomega.4c04577
ACS Omega 2024, 9, 34008−34020

therapy? *Arch. Dermatol. Res.* **2007**, *298* (9), 413−420. Published Online: Nov. 8, 2006.
(30) Pannone, M. C.; Macosko, C. W. Kinetics of isocyanate amine reactions. *J. Appl. Polym. Sci.* **1987**, *34* (7), 2409−2432.
(31) Soucasse, A.; Jourdan, A.; Edin, L.; Gillion, J. F.; Masson, C.; Bege, T. A better understanding of daily life abdominal wall mechanical solicitation: Investigation of intra-abdominal pressure variations by intragastric wireless sensor in humans. *Med. Eng. Phys.* **2022**, *104*, No. 103813. Published Online: Apr. 27, 2022.
(32) Junge, K.; Klinge, U.; Prescher, A.; Giboni, P.; Niewiera, M.; Schumpelick, V. Elasticity of the anterior abdominal wall and impact for reparation of incisional hernias using mesh implants. *Hernia* **2001**, *5* (3), 113−118.
(33) Fatehi Hassanabad, A.; Zarzycki, A. N.; Jeon, K.; Deniset, J. F.; Fedak, P. W. M. Post-Operative Adhesions: A Comprehensive Review of Mechanisms. *Biomedicines* **2021**, *9* (8), 867.
(34) Brandes, R.; Lang, F.; Schmidt, R. F. *Physiologie des Menschen: mit Pathophysiologie*; Springer: Berlin Heidelberg, 2019. DOI: .
(35) Roksnoer, L. C. W.; Heijnen, B. F. J.; Nakano, D.; Peti-Peterdi, J.; Walsh, S. B.; Garrelds, I. M.; Van Gool, J. M. G.; Zietse, R.; Struijker-Boudier, H. A. J.; Hoorn, E. J.; Danser, A. H. J. On the Origin of Urinary Renin: A Translational Approach. *Hypertension* **2016**, *67* (5), 927−933. Published Online: Feb. 29, 2016.
(36) Lih, E.; Oh, S. H.; Joung, Y. K.; Lee, J. H.; Han, D. K. Polymers for cell/tissue anti-adhesion. *Prog. Polym. Sci.* **2015**, *44*, 28−61.
(37) Singh, A. K. Structure, Synthesis, and Application of Nanoparticles. In *Engineered Nanoparticles*; Elsevier, 2016; pp 19−76. DOI: .
(38) Xiao, K.; Wang, Z.; Wu, Y.; Lin, W.; He, Y.; Zhan, J.; Luo, F.; Li, Z.; Li, J.; Tan, H.; Fu, Q. Biodegradable, anti-adhesive and tough polyurethane hydrogels crosslinked by triol crosslinkers. *J. Biomed. Mater. Res., Part A* **2019**, *107* (10), 2205−2221. Published Online: Jun. 6, 2019.
(39) Yu, H. C.; Zhang, H.; Ren, K.; Ying, Z.; Zhu, F.; Qian, J.; Ji, J.; Wu, Z. L.; Zheng, Q. Ultrathin κ-Carrageenan/Chitosan Hydrogel Films with High Toughness and Antiadhesion Property. *ACS Appl. Mater. Interfaces* **2018**, *10* (10), 9002−9009. Published Online: Feb. 28, 2018.
(40) Chou, P. Y.; Chen, S. H.; Chen, C. H.; Chen, S. H.; Fong, Y. T.; Chen, J. P. Thermo-responsive in-situ forming hydrogels as barriers to prevent post-operative peritendinous adhesion. *Acta Biomater.* **2017**, No. 63, 85−95. Published Online: Sep. 12, 2017.
(41) Solbu, A. A.; Caballero, D.; Damigos, S.; Kundu, S. C.; Reis, R. L.; Halaas, Ø.; Chahal, A. S.; Strand, B. L. Assessing cell migration in hydrogels: An overview of relevant materials and methods. *Mater. Today Bio* **2023**, *18*, No. 100537. Published Online: Dec. 29, 2022.
(42) Kim, S. Y.; Shin, M.-S.; Kim, G. J.; Kwon, H.; Lee, M. J.; Han, A.-R.; Nam, J.-W.; Jung, C.-H.; Kang, K. S.; Choi, H. Inhibition of A549 Lung Cancer Cell Migration and Invasion by Ent-Caprolactin C via the Suppression of Transforming Growth Factor-β-Induced Epithelial-Mesenchymal Transition. *Mar. Drugs* **2021**, *19* (8), 465.

https://doi.org/10.1021/acsomega.4c04577
ACS Omega 2024, 9, 34008−34020